

CROSS-RELAXATION EFFECTS IN A RUBY *L*-BAND (1440 Mc/s) MASER AT LOW MAGNETIC FIELDS

By G. S. BOGLE* and F. F. GARDNER†

[Manuscript received February 28, 1961]

Summary

The reversals of maser behaviour which occur in ruby at low fields on cooling from 80° to 4 °K are explained in terms of cross-relaxation transitions (resonant interchanges of energy between neighbouring paramagnetic ions). For an angle of 29° between the magnetic field and the crystal axis a cross-relaxation process has been demonstrated which involves groups of three ions and has a transition probability of 700 ± 100 per second in 0.013% ruby. The profile of the cross-relaxation resonance has a half-width of 190 ± 30 Mc/s at half-intensity, and has an approximately Gaussian shape. It should be possible to obtain useful low-field *L*-band maser action at 4 °K by pumping ν_{41} with the magnetic field nearly perpendicular to the crystal axis, and also at 80 °K using a concentration ten times higher, i.e. 0.13%

I. INTRODUCTION

Since Bloembergen's (1956) original proposal of the three-level solid-state maser a variety of phenomena have been discovered which have clearly demonstrated that processes other than spin-lattice relaxations play a part in determining populations of different states at low temperatures. For example, Autler and McAvoy (1958) found that a maser would not work if the concentration of the active spins was raised above a certain value.

Recently Bloembergen *et al.* (1959) have described a cross-relaxation mechanism which is capable of explaining some of the effects and have applied it in detail to maser action in potassium chromicyanide. The essence of the cross-relaxation process is that two or more neighbouring paramagnetic ions (herein-after called spins) make simultaneous transitions owing to their mutual interaction. The quantum-mechanical treatment of Bloembergen *et al.* shows that the process has highest probability when the total energy of the participating spins is unchanged by their simultaneous transitions.

The probability of the cross-relaxation process depends only on the distances between neighbours and on their quantum-mechanical states and so is nearly independent of temperature. On the other hand the spin-lattice relaxation probabilities are sharply temperature dependent, and it can happen that at 4 °K cross-relaxations occur at a much higher rate than spin-lattice relaxations and will in a maser system radically influence the level populations. In this way, as

* Division of Physics, C.S.I.R.O., University Grounds, Chippendale, N.S.W.

† Division of Radiophysics, C.S.I.R.O., University Grounds, Chippendale, N.S.W.

Shapiro and Bloembergen (1959) have explained, *L*-band maser action in dilute potassium chromicyanide is destroyed when, by adjustment of magnetic field and orientation, two energy gaps are made equal so that double spin-flips may occur without change of total energy.

In this paper we report experiments on an *L*-band (1440 Mc/s) ruby maser. We shall show that cross relaxations involving triple spin-flips are capable of explaining how, under some conditions, maser action which is present at 80 °K deteriorates on cooling and is reversed at 4 °K. Effects of double spin-flips will also be described and discussed.

Mimms and McGee (1960) have also observed triple spin-flips in ruby, using a monitoring frequency of 7170 Mc/s. They have shown that two distinct relaxation times (cross-relaxation and spin-lattice) are exhibited by the spin system when it returns to equilibrium after having been disturbed. On the other hand we have studied, under steady-state conditions, the combined effect of the two kinds of relaxation. By varying temperature (i.e. by changing the spin-lattice relaxation rate) we have been able to distinguish the cross-relaxation processes and measure their rate.

II. ENERGY LEVELS OF Cr^{3+} IN RUBY AT LOW FIELDS

Ruby consists of corundum, $\alpha\text{-Al}_2\text{O}_3$, with a small proportion of the diamagnetic Al^{3+} ions replaced by paramagnetic Cr^{3+} . In most maser work the atomic concentration of chromium is between 0.01 and 0.1%.

The energy levels of Cr^{3+} in ruby are the eigenvalues of an operator called the spin Hamiltonian (see, for example, Bowers and Owen 1955), which is of the form

$$\mathcal{H} = D(S_z^2 - 5/4) + g\beta B.S,$$

where D is a constant, g is the spectroscopic splitting factor (analogous to the Landé g factor of optical spectroscopy), β is the Bohr magneton, S the spin operator, and B the applied magnetic flux density. S has the value 3/2, and there are four distinct energy levels except at zero magnetic field, when they consist of two degenerate doublets separated by $2D$. One doublet, at energy D , corresponds to the eigenstates with $S_z = \pm 3/2$, z being the axis of symmetry of the ruby crystal structure, and the other doublet, at $-D$, to $S_z = \pm 1/2$. In ruby, D is negative, so that the $\pm 1/2$ doublet lies higher in energy; the zero-field splitting frequency $2|D|/h$ is 11.47 Gc/s at low temperatures (Kikuchi *et al.* 1959).

At low magnetic fields, i.e. fields such that $g\beta B$ is small compared with $|D|$, the energies may be calculated by perturbation theory as a function of magnetic field strength (B) and its inclination (θ) to the crystalline axis:

$$\begin{aligned} E_{1,2} &= -|D| \mp \frac{3}{2}g\beta B \cos \theta - \frac{3}{8}(g\beta B \sin \theta)^2/|D|, \\ E_{3,4} &= |D| \mp \frac{1}{2}g\beta B(1 + 3 \sin^2 \theta)^{\frac{1}{2}} + \frac{3}{8}(g\beta B \sin \theta)^2/|D|. \end{aligned} \quad (1)$$

The errors in the above equations are of order $(g\beta B)^3/D^2$. The levels are shown for several values of θ in Figure 1. From a consideration of radiation-induced transition probabilities (see, for example, Howarth 1958 or Weber 1959), it is

found that the transition between levels 4 and 3 is the one most suited for amplification in an *L*-band maser at low fields. To achieve amplification (see below) it is necessary to irradiate the ruby strongly at the frequency $\nu_{42} = (E_4 - E_2)/h$ or ν_{41} , a process called "pumping at ν_{42} or ν_{41} ".

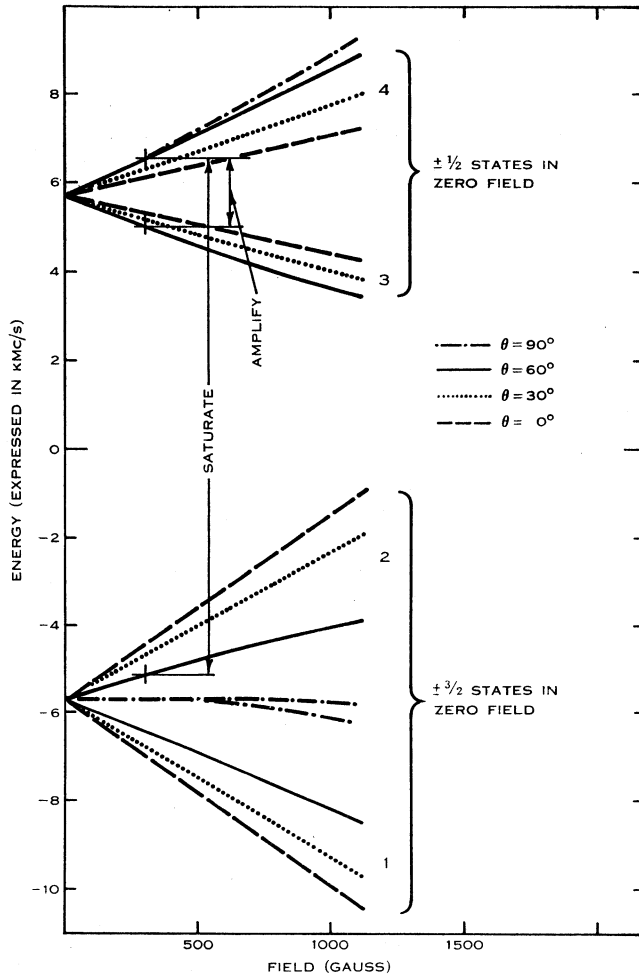


Fig. 1.—Ruby energy levels in low fields for several values of θ , the angle between the magnetic field and the crystalline axis. (For 90° , level 3 is not drawn separately because it is practically the same as for 60° .)

The most natural situation in maser experiments is that ν_{43} is fixed by the dimensions of a cavity resonator, but that a variety of angles, fields, and pumping frequencies are used. Figure 2 shows the values of ν_{41} , ν_{42} , ν_{31} , and B as a function of θ when B is always adjusted to keep the amplifying frequency ν_{43} at 1440 Mc/s ; these have been calculated from equation (1). The figure also shows the variation of ν_{21} , which is relevant to the cross-relaxation processes.

In the discussion of cross-relaxation processes which is given below it will be shown that particular interest attaches to the angles at which ν_{21}/ν_{43} , i.e. $3 \cos \theta / (1 + 3 \sin^2 \theta)^{1/2}$, is an integer.

(i) For $\nu_{21}/\nu_{43}=2$, $\theta=29.2^\circ$. At this angle the total energy of three spins is unchanged by a cross-relaxation process in which two spins jump from levels 4 to 3 and one jumps from 1 to 2.

(ii) For $\nu_{21}/\nu_{43}=1$, $\theta=54.7^\circ$. At this angle the total energy of two spins is unchanged by one spin jumping from 4 to 3 and the other from 1 to 2.

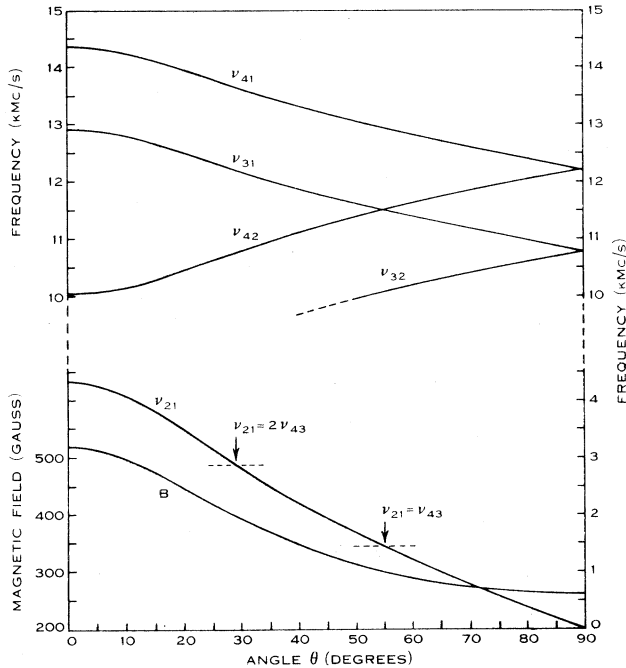


Fig. 2.—Variation of magnetic field and resonant frequencies with angle θ when ν_{43} is maintained at 1440 Mc/s.

III. MASER BEHAVIOUR WITHOUT CROSS RELAXATION

We shall give here a brief recapitulation of Bloembergen's (1956) theory of the three-level paramagnetic maser, before going on to allow for the effect of cross relaxations.

(a) System in Thermal Equilibrium

For the sake of definiteness we consider a Cr^{3+} ion with four energy levels of which the populations are n_1 , n_2 , n_3 , and n_4 , totalling N . In thermodynamic equilibrium $n_j/n_i = \exp(-E_{ji}/kT)$ where $E_{ji} = E_j - E_i$ and k is Boltzmann's constant. Owing to the presence of lattice vibrations, spins continually jump from level to level with a transition probability w_{ij} , w_{ji} , etc. These jumps are called spin-lattice relaxations, and w_{ij} is a spin-lattice relaxation rate. In view of the principle of detailed balancing $n_i w_{ij} = n_j w_{ji}$, whence $w_{ij} = w_{ji} \exp(-E_{ji}/kT)$. The spin-lattice relaxations constitute the mechanism by which the spin system,

when undisturbed, takes up the same temperature as the lattice. In ruby, typical values of w_{ij} are 10^4 and 10 s^{-1} at liquid air and liquid helium temperatures respectively.

(b) *System with Microwave Radiation*

When the microwave frequency is at or near a resonant frequency of the system, namely, $\nu_{ji} = (E_j - E_i)/h$, radiation-induced transitions occur from the level i to j , and vice versa, with the common transition probability W_{ij} . (For the moment, we suppose that $E_j > E_i$). W_{ij} is proportional to the incident power P , and the absorption of power is described by the equation

$$-dP = (n_i - n_j)h\nu_{ji}W_{ij}. \quad (2)$$

The absorption coefficient is thus proportional to $n_i - n_j$, and this fact is used to monitor changes of $n_i - n_j$ which may occur when the system is disturbed as in a maser.

For large power such that $W_{ij} \gg w_{ij}$, w_{kl} , etc., the power absorbed no longer increases in proportion to incident power but reaches a limit imposed by the spin-lattice relaxation rates. Thus the absorption coefficient and the population difference $n_i - n_j$ both tend to zero. This is the phenomenon of "saturation of the resonance line" well known in microwave spectroscopy.

To operate a maser of the Bloembergen type, a system of energy levels, such as is shown in Figure 1, is used. The amplification frequency is chosen to correspond to one of the smaller energy splittings such as $E_4 - E_3$, and strong microwave power is applied at one of the high frequencies such as ν_{42} in order to saturate the resonance. When the pumping power is applied the population difference, in this case $n_3 - n_4$, becomes reversed in sign so that, according to equation (2), power applied at ν_{43} is amplified instead of being absorbed.

This population change may be calculated by the method of Bloembergen, and we quote the results below; but it may also be understood by means of a simple geometric treatment which is modelled on that of Geusic *et al.* (1959).

(c) *Qualitative Treatment of Maser Action*

Let the populations n_i , which are proportional to $\exp(-E_i/kT)$, be plotted as ordinate with energy as abscissa (Fig. 3 (a)). In the "high temperature approximation" always made in maser calculations, all energies are assumed small compared to kT , so that for all levels $\exp(-E_i/kT) \simeq 1 - E_i/kT$ and the populations are given by $n_i \simeq \frac{1}{2}N[1 - (E_i - E_m)/kT]$, where E_m is the mean energy. This is a fairly good approximation in the present case where the highest frequency involved is about 15 kMc/s, since 4° K , the lowest temperature used, is equivalent to about 100 kMc/s. In this approximation a straight line with slope $-N/(4kT)$ may be drawn through the points n_1 to n_4 of Figure 3 (a).

Figure 3 (b) represents the effect of pumping at ν_{42} . The populations n_3 and n_4 have each been replaced by $n'_4 = n'_2 = \frac{1}{2}(n_2 + n_4)$. It may be seen by inspection of the figure that if $\nu_{42} \gg \nu_{43}$ the population of the upper level E_4 exceeds that of E_3 , so that maser action is possible at the frequency ν_{43} . Indeed, a simple calculation from the figure shows that the population excess is $(N\hbar/4kT)(\frac{1}{2}\nu_{42} - \nu_{43})$.

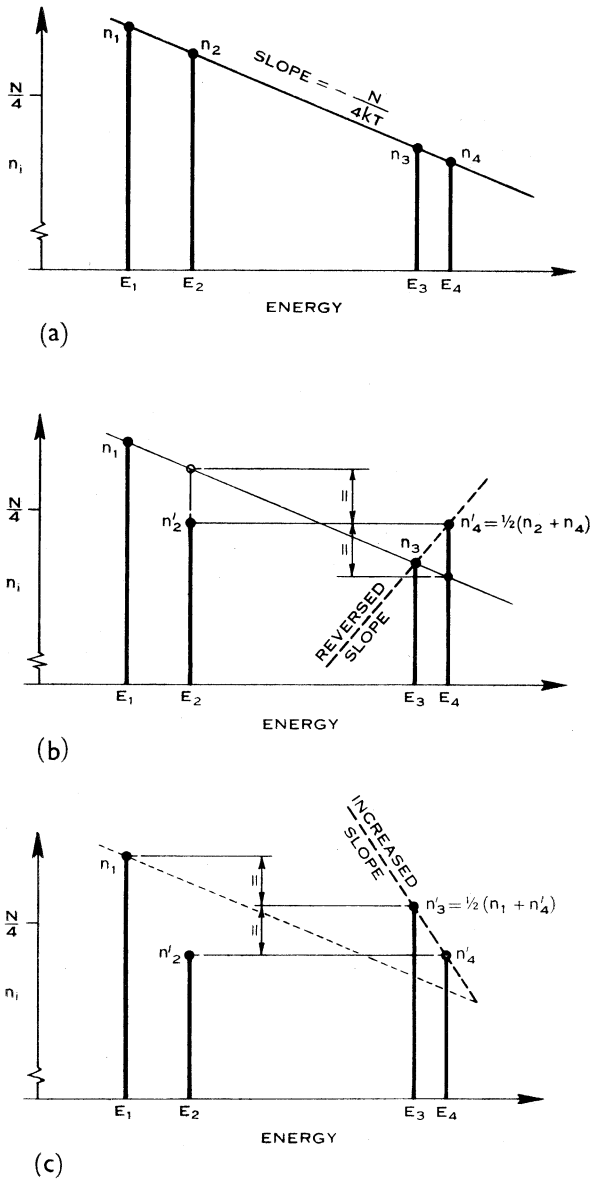


Fig. 3.—Level populations (a) in thermal equilibrium, (b) when ν_{42} is saturated, equalizing n_2 and n_4 , and (c) when in addition a cross-relaxation process is present which makes n_3 equal to the mean of n_1 and n_4 .

The natural quantity to measure in experiments is the ratio, with and without pumping, of the strengths of the resonance line at ν_{43} (treating an emission line as a negative absorption line). This, in turn, is equal to the ratio of the corresponding population differences, which we call Δn_{34} and $\Delta_0 n_{34}$ with and without pumping. Thus the maser equation is most conveniently written in terms of the ratio $\Delta n_{34}/\Delta_0 n_{34}$, and in the present case becomes

$$\Delta n_{34}/\Delta_0 n_{34} = 1 - \frac{1}{2} \nu_{42}/\nu_{43}. \quad (3)$$

(d) *Results of the Quantitative Theory of Maser Action*

The solution for a system of three levels has been given by Bloembergen (1956) and that for four levels, which is not different in principle, has been given, for example, by Bogle and Symmons (1959). Adapting level labels to the present case we obtain

$$\frac{\Delta n_{34}}{\Delta_0 n_{34}} = 1 - \frac{\nu_{42}}{\nu_{43}} \cdot \frac{w_1 w_{23} + w_{13} w_{12}}{w_1(w_{23} + w_{34}) + w_{13}(w_{12} + w_{14})}, \quad (4a)$$

where $w_1 = w_{12} + w_{13} + w_{14}$. (Owing to the nature of the approximations made there is no need to distinguish between w_{ij} and w_{ji} .) Some justification for the "geometric" calculation based on Figure 3 (b) is afforded by the fact that equation (4a) reduces to (3) when all the w_{ij} are the same.

Equation (4a) may be adapted for pumping ν_{41} instead of ν_{42} simply by interchanging the suffices 1 and 2, yielding

$$\frac{\Delta n_{34}}{\Delta_0 n_{34}} = 1 - \frac{\nu_{41}}{\nu_{43}} \cdot \frac{w_2 w_{31} + w_{23} w_{21}}{w_2(w_{31} + w_{34}) + w_{23}(w_{21} + w_{24})}. \quad (4b)$$

The expected value of $\Delta n_{34}/\Delta_0 n_{34}$ for a 1400 Mc/s maser, assuming equal w_{ij} 's, is about -3 at all angles whether ν_{42} or ν_{41} is pumped. We shall call this "a maser effect of 3".

If the pumping frequency is changed to ν_{31} it is easy to see, from a diagram like that of Figure 3 (b), that Δn_{34} is larger than $\Delta_0 n_{34}$, so that the absorption coefficient is increased. We call this "an antimaser effect". The corresponding equation may easily be derived from (4a) by changing level labels and remembering that the ν_{ij} are signed quantities (i.e. that $\nu_{ij} = -\nu_{ji}$). The result is

$$\frac{\Delta n_{34}}{\Delta_0 n_{34}} = 1 + \frac{\nu_{31}}{\nu_{43}} \cdot \frac{w_2 w_{14} + w_{24} w_{12}}{w_2(w_{14} + w_{34}) + w_{24}(w_{12} + w_{23})}, \quad (5)$$

where $w_2 = w_{21} + w_{23} + w_{24}$. A similar equation holds for pumping at ν_{32} , and for either ν_{31} or ν_{32} the antimaser effect should be about 5, with only slight dependence on angle.

When $\theta = 90^\circ$, levels 1 and 2 nearly coincide: their separation is only a few megacycles per second, whereas their widths are about 60 Mc/s. Thus pumping at ν_{42} inevitably implies pumping at ν_{41} , and, similarly, pumping at ν_{31} and ν_{32} are inseparable. This produces stronger maser and antimaser effects. For pumping at ν_{42} and ν_{41} ($=\nu_p$) the equation becomes

$$\frac{\Delta n_{34}}{\Delta_0 n_{34}} = 1 - \frac{\nu_p}{\nu_{43}} \cdot \frac{w_{13} + w_{23}}{w_{13} + w_{23} + w_{43}}, \quad (6)$$

and, for pumping ν_{31} and ν_{32} ($=\nu_p$),

$$\frac{\Delta n_{34}}{\Delta_0 n_{34}} = 1 + \frac{\nu_p}{\nu_{43}} \cdot \frac{w_{14} + w_{24}}{w_{14} + w_{24} + w_{34}}. \quad (7)$$

The important conclusion from the above equations is that if the system is pumped at ν_{42} or ν_{41} the result can *only* be a maser effect (except in the unlikely event that at least two w 's, e.g. w_{23} and w_{12} in equation (4a), are zero); and if pumped at ν_{31} or ν_{32} the result can only be an antimaser effect (unless two w 's such as w_{14} and w_{12} in equation (5) are zero). In fact, at liquid helium temperatures, the opposite is observed: this shows that the picture of maser action presented above is not complete.

IV. EFFECT OF CROSS RELAXATION ON THE LEVEL POPULATIONS

The existence of cross-relaxation processes was first recognized by Bloembergen *et al.* (1959). They showed by a quantum-mechanical treatment that a group of neighbouring spins could execute simultaneous transitions under the influence of their mutual interaction. Figure 4 (a) shows a possible group of three closely neighbouring chromium ions α , β , and γ in a randomly distributed array. The probability of the simultaneous transition is greatest when the total energy of the participants is unchanged: that is, the cross-relaxation process is a type of resonance phenomenon. The conservation of energy need not be exact; there is a "line width" which is expected to be a few times greater than that of the levels themselves, and the latter is about 60 Mc/s in the ruby generally used in masers.

In ruby, with the magnetic field applied at the angle $\theta=29.2^\circ$ to the c -axis, it has been shown above that $2(E_4 - E_3) = E_2 - E_1$. Thus a cross-relaxation process is "on resonance" in which one spin jumps from E_2 to E_1 , while two neighbours jump from E_3 to E_4 . This process is illustrated in Figure 4 (b). The process of Figure 4 (c) is, of course, also on resonance and has the same effect on the level populations. We do not believe the two processes can be distinguished, and in what follows we shall, for clarity, speak in terms of the process of Figure 4 (b).

It is shown in the Appendix that the complete rate equation for, say, level 3 is now

$$\frac{dn_3}{dt} = \sum_{j \neq 3} w_{j3} \left(n_j - n_3 + \frac{N h \nu_{j3}}{4kT} \right) + \sum_{j \neq 3} W_{j3} (n_j - n_3) + 2c^2 w_c (n_1 n_4^2 - n_2 n_3^2) / N^2. \quad (8)$$

The first term on the R.H.S. gives the contribution of the spin-lattice relaxations, the second that of the radiation-induced transitions, and the third that of the cross-relaxation processes. The cross-relaxation coefficient w_c depends on the quantum states of the Cr^{3+} ion and on the lattice spacings, and c is the ionic concentration of Cr^{3+} relative to Al^{3+} . In the steady state, of course, $dn_3/dt=0$.

Equation (8) and its companions may now be solved generally by the method of Shapiro and Bloembergen (1959). (In their notation $c^2 w_c$ would be called w_{124343} .) However, useful qualitative conclusions from equation (8) may readily be drawn. Let the pumping frequency be ν_{42} : then W_{42} is large but all W_{j3} are zero, so that the R.H.S. of equation (8) consists of only two terms. Since

$dn_3/dt=0$, and the first term on the R.H.S. is at most of order $w_{ij}N$, w_{ij} meaning a typical spin-lattice relaxation rate, it follows that

$$|(n_1n_4^2 - n_2n_3^2)/N^3| \simeq w_{ij}/(c^2w_c).$$

If $c^2w_c \gg w_{ij}$, as we believe to be the case in our experiments at liquid helium temperatures (see below), the fractional difference between $n_1n_4^2$ and $n_2n_3^2$ must be very small. One may then treat the cross relaxations as imposing the restraint that $n_1n_4^2 = n_2n_3^2$.

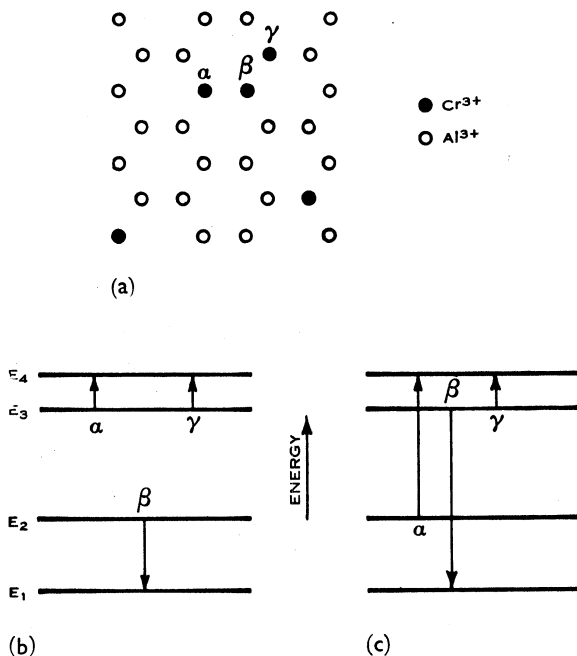


Fig. 4.—(a) Sketch of a small region of ruby crystal showing one of the occasional close groups of paramagnetic ions; (b) and (c) the cross-relaxation processes executed by a group when $E_2 - E_1 = 2(E_4 - E_3)$ as in ruby at $\theta = 29^\circ$.

Consider now the effect of cross relaxations when pumping at ν_{42} . Figure 3 (a) shows the system in equilibrium, Figure 3 (b) shows the effect of the constraint $n_2 = n_4$ which is imposed by pumping at ν_{42} . Because $n_2 = n_4$, the cross-relaxation constraint simplifies to $n_1n_4 = n_3^2$. In other words, n_3 becomes the geometric mean of n_1 and n_4 , or approximately the arithmetic mean, since all n 's are supposed equal to within about $Nh\nu/4kT$. The cross relaxations, then, impose the restraint that $n_3 = \frac{1}{2}(n_1 + n_4)$. The effect of this last constraint is shown in Figure 3 (c). The final population difference $n_3' - n_4'$ is seen to be larger than in thermal equilibrium: in other words, there is an antimaser effect. (Strictly speaking, after n_3 is raised to n_3' all the populations in Figure 3 (c) should be reduced slightly to conserve total population; but this would have no effect on the argument, which is, in any case, only qualitative.)

The above discussion gives a physical picture of the way cross-relaxation processes can, near $\theta=29^\circ$, reverse the maser effect which was expected on the basis of the old maser equations. We shall now give the results of the analytical treatment of the above situation and of others which are important for an understanding of our experiments.

(a) *Cross-relaxation Effects near $\theta=29^\circ$*

At $\theta=29.2^\circ$, $\nu_{21}=2\nu_{43}$; the associated cross-relaxation process has been described immediately above.

(i) *Pumping at ν_{42}* .—For the general case, the solution of the set of equations like (8) leads to the result

$$\frac{\Delta n_{34}}{\Delta_0 n_{34}} = 1 - \frac{\nu_{42}}{\nu_{43}} \cdot \frac{w_1 w_{23} + w_{13} w_{12} + (c^2 w_c / 16)(w_{23} - w_{13} - 2w_{14})}{w_1(w_{23} + w_{34}) + w_{13}(w_{12} + w_{14}) + (c^2 w / 16)(w_3 + 4w_{12} + 4w_{14})}. \quad (9)$$

The reason why $c^2 w_c / 16$, rather than $c^2 w_c$, enters the above equation is that, as shown in the Appendix, $c^2 w_c / 16$ is the quantity which has the same kind of significance as w_{ij} ; that is, $c^2 w_c / 16$ is the rate per ion at which cross relaxations occur.

Three special cases of (9) are of interest.

(1) $c^2 w_c / 16 \ll w_{ij}$'s.

This simply gives the familiar 4-level maser equation of equation (4a).

(2) $c^2 w_c / 16 \gg w_{ij}$'s.

This is the case which has been qualitatively described above by means of Figure 3 (c). The equation is

$$\frac{\Delta n_{34}}{\Delta_0 n_{34}} = 1 + \frac{\nu_{42}}{\nu_{43}} \cdot \frac{2w_{14} + w_{13} - w_{23}}{w_3 + 4w_{12} + 4w_{14}}, \quad (10)$$

which bears out the conclusion of the "geometrical" method of Figure 3 that there is an antimaser effect (except in the unlikely event that $w_{23} > 2w_{14} + w_{13}$).

(3) $c^2 w_c / 16 = 2w_{ij}$.

In this case, provided all the w_{ij} are equal, $\Delta n_{34} / \Delta_0 n_{34} = 1$: that is, the application of pumping power leaves the absorption coefficient at ν_{43} unaffected. If the w_{ij} 's are not equal, the statement holds for some weighted average of the w_{ij} 's which could be computed from equation (9); but this refinement is hardly warranted in the present state of knowledge of the w_{ij} 's.

The variation of the maser effect for other ratios of w_{ij} to $c^2 w_c / 16$ is shown in Figure 5, again assuming equal w_{ij} 's.

(ii) *Pumping at ν_{41}* .—Proceeding as for equation (9), but with the simplification that $c^2 w_c / 16 \gg w_{ij}$'s, we obtain

$$\frac{\Delta n_{34}}{\Delta_0 n_{34}} = 1 - \frac{\nu_{41}}{\nu_{43}} \cdot \frac{3w_{23} + 2w_{24} + w_{13}}{4w_2 + 4w_{23} + w_3}, \quad (11)$$

from which the important conclusion is that a maser effect is produced, just as in the absence of cross relaxations.

(iii) *Pumping at ν_{31} .*—With $c^2w_c/16 \gg w_{ij}$ as before, we obtain

$$\frac{\Delta n_{34}}{\Delta_0 n_{34}} = 1 - \frac{\nu_{31}}{\nu_{43}} \cdot \frac{2w_{23} + w_{24} - w_{14}}{w_4 + 4w_{12} + 4w_{23}} \quad (12)$$

This shows that, except in the unlikely event that $w_{14} > 2w_{23} + w_{24}$, there is a maser effect, contrary to the effect in the absence of cross relaxations.

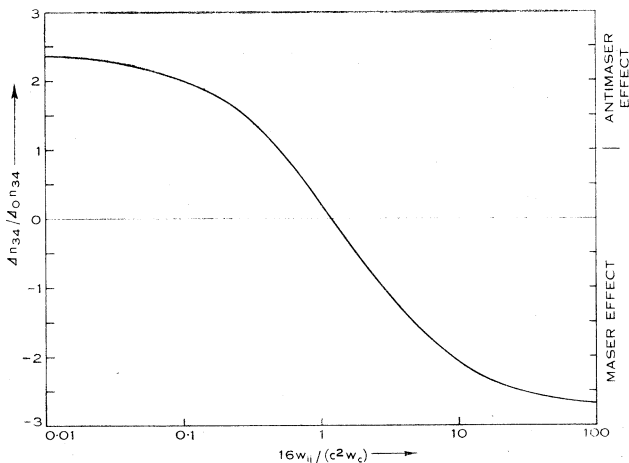


Fig. 5.—Variation of $\Delta n_{34}/\Delta_0 n_{34}$ as a function of the ratio of the spin-lattice relaxation rate w_{ij} to the cross-relaxation rate $c^2w_c/16$. The right-hand side of the diagram corresponds to higher temperature.

(b) *Cross-relaxation Effects near $\theta=55^\circ$*

At this angle $E_4 - E_3 = E_2 - E_1$, and the cross-relaxation process consists in an ion jumping from E_4 to E_3 while a neighbour jumps from E_1 to E_2 . The quantity which must now be added to the rate equation for, say, level 3 is now readily shown to be $cw_c'(n_1n_4 - n_2n_3)/N$, where w_c' is quite distinct from the w_c which has been used for the $\theta=29^\circ$ case.

By the same kind of argument as before it is seen that the cross relaxations tend to equalize n_1n_4 and n_2n_3 . The analysis in this case is very similar to that used by Shapiro and Bloembergen (1959); in their notation cw_c' would be called $w_{12, 43}$.

The expressions given below have all been derived for the case $cw_c' \gg w_{ij}$.

(i) *Pumping at ν_{42} .*—

$$\frac{\Delta n_{34}}{\Delta_0 n_{34}} = 1 + \frac{\nu_{42}}{\nu_{43}} \cdot \frac{w_{14} - w_{23}}{w_{34} + w_{12} + w_{32} + w_{14}} \quad (13)$$

(ii) *Pumping at ν_{41} .*—

$$\frac{\Delta n_{34}}{\Delta_0 n_{34}} = 1 - \frac{\nu_{41}}{\nu_{43}} \cdot \frac{2w_{23} + w_{24} + w_{31}}{2w_{23} + w_2 + w_3} \quad (14)$$

(iii) *Pumping at ν_{31} .*—The result is identical with (13) except that ν_{42} in that equation must be changed to ν_{31} . This identity is easy to understand physically: if the pumping makes $n_2=n_4$, the cross relaxations make $n_1=n_3$, and vice versa. At $\theta=55^\circ$, of course, $\nu_{42}=\nu_{31}$ (Fig. 2).

The equality of ν_{42} and ν_{31} at 55° has another consequence: even if cross relaxations are negligible, pumping at ν_{42} or ν_{31} inevitably makes $n_2=n_4$ and $n_1=n_3$. The resulting equation for $\Delta n_{34}/\Delta_0 n_{34}$ is the same as equation (13). Thus, near 55° , it is difficult experimentally to distinguish whether cross-relaxation processes are dominant or not, when pumping at ν_{42} or ν_{31} .

V. SPIN-LATTICE RELAXATION RATES

The most complete set of measurements of the several w_{ij} 's which has been made appears to be that of Pace, Sampson, and Thorp (1960*a*, 1960*b*). (These authors quote values of the relaxation time T_1 , but in the present discussion they have been converted to the corresponding relaxation rates $w=1/(2T_1)$.) At liquid air temperature it was found that the w_{ij} 's were nearly equal to each other while at liquid helium temperatures those transitions which had relatively low magnetic dipole moments were also found to have relatively low w 's. The measurements were taken at much higher fields than in our experiments; but evidence was quoted that the relaxation rates were not strongly field dependent.

TABLE 1
ASSUMED VALUES OF THE w_{ij} 's AT 4° K ACCORDING TO THE "MAGNETIC
DIPOLE MODEL" WITH FIELD ADJUSTED TO KEEP ν_{43} AT 1440 Mc/s
(ARBITRARY UNITS)

θ	0°	30°	60°	90°
w_{34}	2.0	1.6	1.3	1.2
w_{23}	0.0	0.3	0.6	0.8
w_{12}	0.0	0.0	0.0	2.2
w_{24}	1.5	1.2	0.8	0.7
w_{13}	1.5	1.3	1.0	0.8
w_{14}	0.0	0.3	0.4	0.7

At the present state of knowledge it seems to us that the best course is to assume that at liquid helium temperatures the w_{ij} 's are proportional to the corresponding magnetic dipole transition probabilities, which are given, for example, by Howarth (1958) and Weber (1959). As an added refinement we have averaged the probabilities with regard to direction. The resulting spin-lattice relaxation rates, in arbitrary units, are given for several values of θ in Table 1. The field has been adjusted at each angle to maintain ν_{43} at 1440 Mc/s. We shall call this the "magnetic dipole model" of spin-lattice relaxation rates.

We also require the temperature variation of the spin-lattice relaxation rates. We have made measurements at several temperatures in the liquid oxygen and liquid helium ranges, by measuring the decay of the maser effect when the pumping power is switched off. The results are shown in Figure 6, together with

those of Pace, Sampson, and Thorp (1960*a*, 1960*b*). The two curves taken together strongly confirm the conclusion of those authors that there is only slight dependence of relaxation rate on microwave frequency, in contrast to the theoretically predicted variation as ν^2 or ν^4 (Van Vleck 1940). The transition concerned in our relaxation measurements was that between the levels 3 and 4

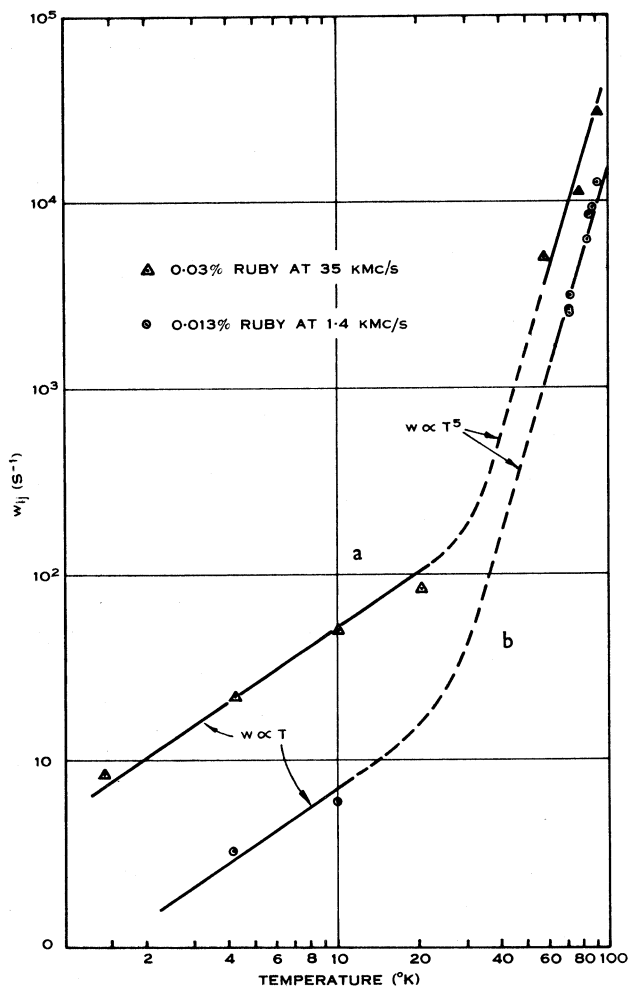


Fig. 6.—Measured and interpolated temperature-variation of the spin-lattice relaxation rate in ruby (a) at 35 kMc/s with 0.03% concentration (Pace, Sampson, and Thorp 1960*a*, 1960*b*); (b) at 1.4 kMc/s with 0.013% concentration (present work).

(i.e. between the $\pm 1/2$ states) and θ was 35° at liquid air temperatures (because this angle happened to favour strong pumping) and 90° at liquid helium temperatures (chosen in order to minimize cross-relaxation effects). It is true that the T^5 and T variations shown in the figure are not conclusively established by our own measurements but they are strongly suggested when the latter are taken together

with the results of Pace, Sampson, and Thorp. Moreover, it will be seen below that this temperature variation is consistent with the observations of the change of the maser effect with temperature.

VI. EXPERIMENTAL BEHAVIOUR OF THE LOW-FIELD MODES

(a) *Experimental Procedure*

The experiments were carried out at temperatures between 4° and 90 °K with an *X*-band waveguide cavity containing an *L*-band quarter-wave strip-line resonator. The *L*-band frequency was fixed at 1440 Mc/s but a multiplicity of cavity resonances permitted a number of *X*-band pumping frequencies between 10 and 14 kMc/s to be used. (Strictly speaking, the frequencies from 12·4 to 14 kMc/s do not belong to *X*-band, but we shall use the term “*X*-band” for all our pumping frequencies.) Using a 50 c/s magnetic sweep, the *L* and *X* para-

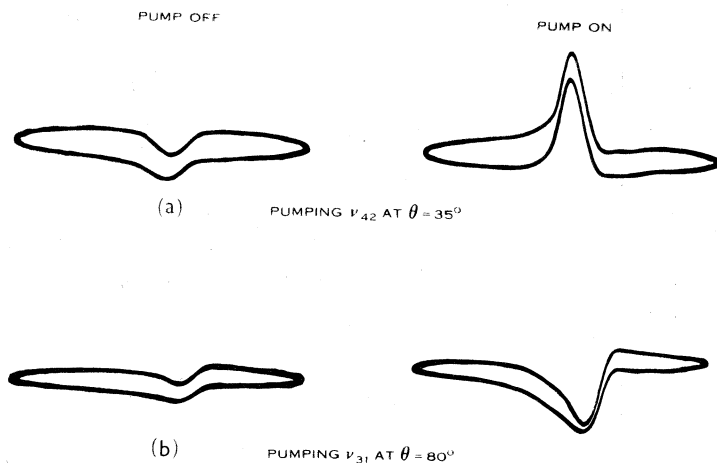


Fig. 7.—Examples of (a) maser and (b) antimaser effects at 80 °K, pumping at 10·9 kMc/s. The magnetic sweep is 140 gauss peak-to-peak at 50 c/s and a downward dip corresponds to absorption. (The separation between the forward and backward traces is due to 50 c/s pick-up, and the asymmetry in (b) is due to a slight detuning of the *L*-band oscillator from the cavity resonant frequency).

magnetic resonance lines could be displayed together on a double-beam oscilloscope. With the magnitude and orientation of the d.c. magnetic field adjusted so that the resonances coincided in field, the ratio of strengths of the 1440 Mc/s resonance with and without *X*-band pumping was noted. This ratio is equal to $\Delta n_{34}/\Delta_0 n_{34}$. Figure 7 shows examples

- (a) of stimulated emission or maser effect where $\Delta n_{34}/\Delta_0 n_{34}$ is negative, and
- (b) of enhanced absorption or antimaser effect where $\Delta n_{34}/\Delta_0 n_{34}$ is positive and greater than unity.

The concentration of Cr^{3+} in the ruby used was found by comparing its paramagnetic resonance intensity with that of a weighed sample of $\text{CuSO}_4 \cdot 5\text{H}_2\text{O}$. The atomic concentration of Cr^{3+} relative to Al^{3+} was estimated to be $0\cdot013 \pm 0\cdot003\%$.

Temperatures were measured with both a carbon resistor and a copper-constantan thermocouple, and the various temperatures between 4 and 60 °K were obtained sometimes by siphoning limited amounts of liquid helium into the cryostat and sometimes by following the slow warm-up of the cryostat after the evaporation of a charge of liquid helium. The temperature measurements in the above range are considered accurate to about ± 3 °K.

Because of the cut of the ruby used the angles θ available were limited to the range 20°–90°.

(b) *Behaviour at Liquid Air Temperature*

Maser effects are observed at all angles when pumping with ν_{41} or ν_{42} . With ν_{42} , the values of $\Delta n_{34}/\Delta_0 n_{34}$ are about -3 , which is in agreement with the prediction of equation (4a). When ν_{31} is pumped, antimaser effects are observed with a magnitude typically of $+4$, in reasonable agreement with equation (5), which predicts $+5$.

(c) *Observations at Liquid Helium Temperatures*

There are now considerable variations with angle and we present the results in Figure 8 (pumping ν_{42} and ν_{41}) and Figure 9 (ν_{31}).

The essential features predicted by the cross-relaxation theory are exhibited. Near $\theta=29^\circ$ both the ν_{42} and ν_{31} curves show the reversals which are predicted in equations (10) and (12). Near $\theta=55^\circ$ they both show absence of any strong effect as predicted by equation (13), though (as discussed already in Section IV (b) (iii)) this is not definite evidence for a 55° cross-relaxation process. The curve for ν_{41} shows no maser reversal, which is in accordance with equations (11) and (14). The singularity in this curve at $\theta=55^\circ$ is good evidence of the influence of the 55° cross-relaxation process.

The intensification of all effects at $\theta=90^\circ$, which is expected from equations (6) and (7), is also clearly apparent. This is a consequence not of cross relaxation but, as has already been shown in Section III (d), of double pumping.

However, the quantitative predictions of the theory are not borne out by experiment. In Table 2 we compare the measured values of $\Delta n_{34}/\Delta_0 n_{34}$ with the predictions of the theory using both the magnetic dipole model of spin-lattice relaxation rates and the "homogeneous model" in which they are all equal.

The table shows that the actual effects are all smaller than expected from the theory. A possible explanation is that the w_{ij} 's are very different from those of either model. If, for example, at $\theta=29^\circ$ the w_{ij} 's had the values given in Table 1 except that $w_{34}+4w_{12}=15$, then the theoretical ratios $\Delta n_{34}/\Delta_0 n_{34}$ would become 1.7, -0.8 , and 0.3 for pumping at ν_{42} , ν_{41} , and ν_{31} respectively (experiment: 1.6, -0.6 , 0.0). However, we believe that the true explanation is that at 4 °K a variety of other cross-relaxation processes, although not "on resonance", have nevertheless attained an influence comparable to that of the spin-lattice relaxations. This situation has also been inferred by Mimms and McGee (1960), who have called it "general cross relaxation". If the temperature were lowered further still (or the concentration raised) the situation would approach that discussed by Shapiro and Bloembergen (1959). They have shown that when the concentration is high enough the spin system as a whole

warms up if any resonance is pumped: that is, $\Delta n_{34}/\Delta_0 n_{34}$ tends to zero, and maser action is impossible. Our case is less extreme; but it may be seen from Figure 8 that the effects are indeed diminishing as temperature is lowered. It appears that at about 20 °K the behaviour of 0.013% ruby would exemplify much better the theory presented in this paper. For example, near 20 °K and at $\theta=29^\circ$ the observed effect when pumping ν_{42} is +2.3 (theory, +2.4); and at $\theta=55^\circ$ pumping ν_{41} the effect is -2.4 (theory, -3.5).

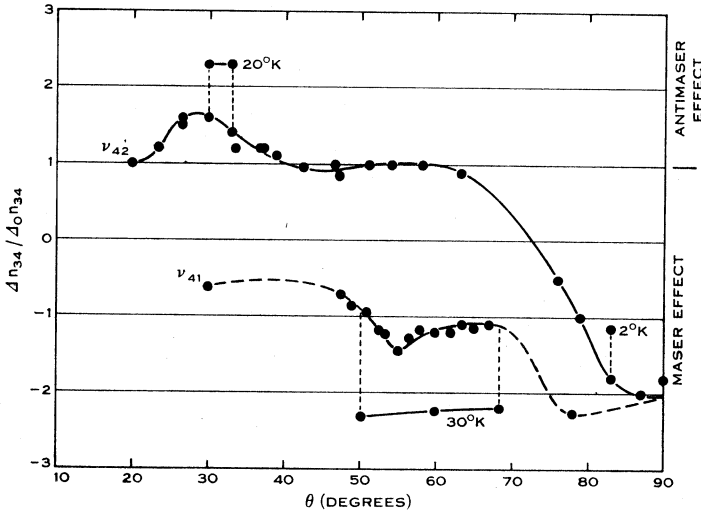


Fig. 8.—Maser and antimaser effects as a function of orientation when pumping at ν_{42} and ν_{41} . The temperature is 4 °K except where otherwise noted.

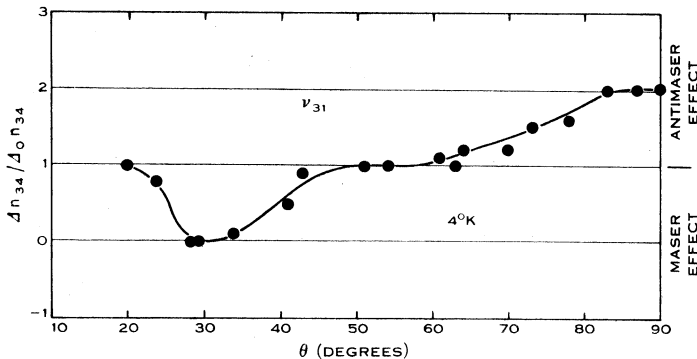


Fig. 9.—Variation of $\Delta n_{34}/\Delta_0 n_{34}$ with angle when ν_{31} is pumped at 4 °K.

(d) Temperature Dependence of the Maser Effect

It has been seen above that when the pumping frequency is ν_{42} and the angle θ is near 29° the maser effect reverses on cooling from liquid air to liquid helium temperatures. In Figure 10 we give tracings from oscilloscope photographs which show this change for $\theta=33^\circ$. (These were taken in the early stages of the experiments when the L-band detector was a travelling-wave amplifier

which was unduly susceptible to microphonic disturbances: the majority of our results have been obtained with a superheterodyne receiver which was much superior in this respect, as comparison of Figures 10 and 7 shows.)

During the course of the experiments a number of observations were made of the ratio $\Delta n_{34}/\Delta_0 n_{34}$ at various angles θ near 29° and various temperatures between 4 and 80°K . Many of these are plotted as points in Figure 11. The points plotted as full circles are for θ close to its resonance value of 29° ; and those as open circles and triangles for θ off-resonance by the amounts labelled. The curves have been calculated, choosing the value of $c^2 w_c/16$ which gives the best fit, by combining the information given by Figures 5 and 6. It may be seen that the on-resonance points are in good agreement with the theory with $c^2 w_c/16=700/\text{s}$ and the 4° off-points with $c^2 w_c/16=180/\text{s}$. This statement is

TABLE 2
VALUES OF $\Delta n_{34}/\Delta_0 n_{34}$ AT 4°K

Angle	$\Delta n_{34}/\Delta_0 n_{34}$		
	From Dipole Model	from Homogeneous Model	Experiment
	<i>Pumping ν_{42}</i>		
29	+3.7	+2.4	+1.6
55	+0.5	+1.0	+1.0
90	-3.8	-4.7	-2.0
	<i>Pumping ν_{41}</i>		
29	-3.3	-2.0	-0.6
55	-3.8	-3.5	-1.5
90	-3.8	-4.7	-2.0
	<i>Pumping ν_{31}</i>		
29	-3.0	-0.5	0.0
55	+0.5	+1.0	+1.0
90	+5.0	+6.0	+2.0

true of the change-over temperature region where the maser reversal is most rapid, and this fact increases our confidence in the assumptions underlying Figures 5 and 6 and in the values of $c^2 w_c/16$ deduced above. At helium temperatures the agreement is worse than appears from Figure 11 because the use of the magnetic dipole model of the w_{ij} 's, which should be a better approximation than the homogeneous model used for Figures 5 and 11, predicts an antimaser effect of nearly 4 as against the observed 1.6. We have already discussed how this effect is probably due to the participation of other cross-relaxation processes not on resonance ("general cross relaxation").

(e) Profile of the 29° Cross-relaxation Process

In the last section we have shown that the cross-relaxation rate $c^2 w_c/16$ falls from 700 to 180/s when θ is taken off-resonance by $\pm 4^\circ$. Now it can easily be shown that between $\theta=20$ and 40° the change of $2\nu_{43}-\nu_{21}$ is practically linear with angle, the slope being 63 Mc/s per degree, under the conditions of the

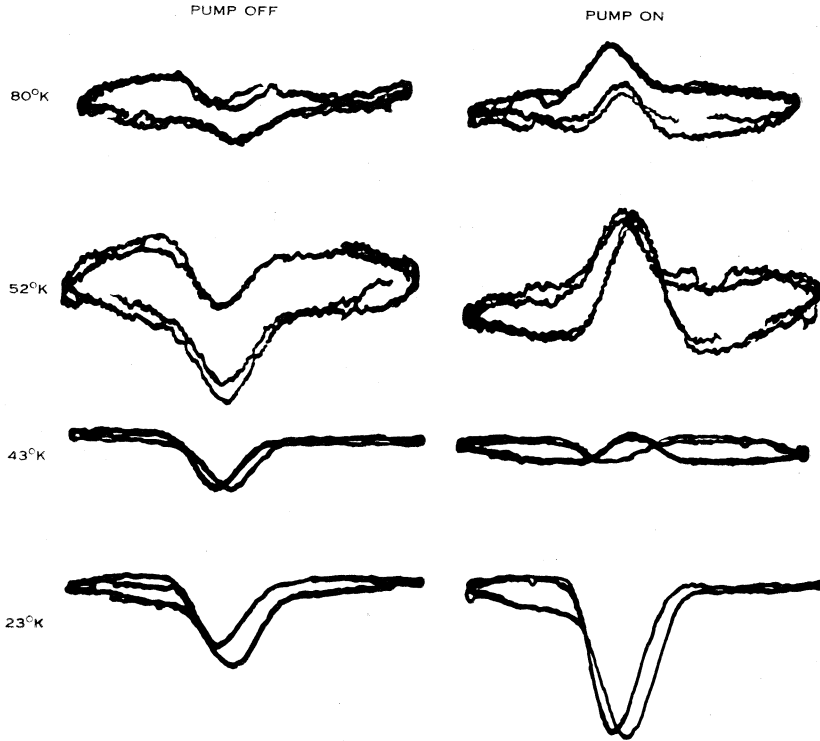


Fig. 10.—Maser reversal on cooling. The pumping frequency is ν_{42} and the angle 33° , and the method of display is the same as for Figure 7.

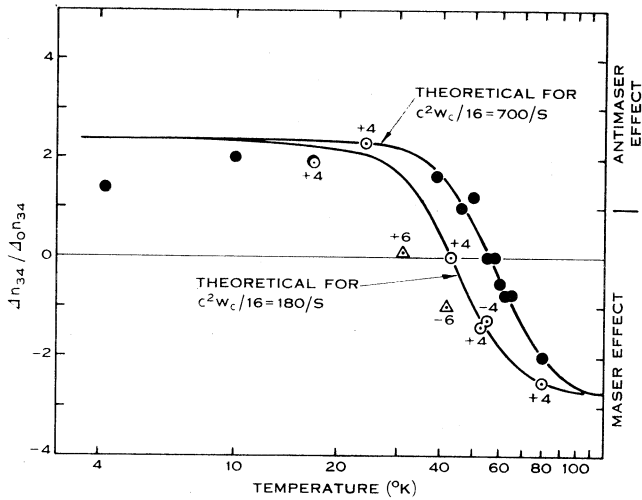


Fig. 11.—Maser reversal on cooling : values of $\Delta n_{34} / \Delta_0 n_{34}$ for pumping at ν_{42} with θ near 29° . The points are labelled with the values of $\theta - 29$ where this difference is greater than one degree.

hydrogen temperatures the individual 29° and 55° cross-relaxation effects would be manifested as strongly as predicted. For the $\theta=29^\circ$ process the cross-relaxation term $c^2w_c/16$, which enters equation (9), has been found to have the value 700 s^{-1} in ruby with 0.013% chromium ion concentration. If the concentration were increased tenfold (to 0.13%) the cross-relaxation rate $c^2w_c/16$ would increase to $7 \times 10^4\text{ s}^{-1}$, and it may be seen using Figures 5 and 6 that strong anomalous maser effects would be observed at liquid air temperatures.

(ii) A method has been demonstrated for measuring the profile of the cross-relaxation process at $\theta=29^\circ$. This could be developed to give much greater precision by constructing equipment in which the pumping frequency could be varied continuously and the temperature maintained at steady values between liquid air and liquid helium temperatures.

(iii) As regards the operation of low-field ruby masers the best conditions appear (cf. Fig. 8) to be at $\theta \approx 80^\circ$ with pumping at ν_{41} , i.e. at about 12.4 Gc/s in the case of an L -band maser. The concentration of 0.013% is not necessarily the best for 4°K operation. It appears that the low-field L -band maser has been hitherto unjustly neglected, for the inversion ratio is nearly half as great as in the more developed 2000 gauss type (Arams and Okwit 1959), and the amplifying transition is of comparable intensity and is more nearly circularly polarized. Useful maser action should also be obtainable at liquid air temperature, for the loss of performance associated with the twentyfold increase of temperature could be largely offset by a tenfold increase of chromium concentration.

(iv) The cross-relaxation measurements have an important bearing on the phenomenon of "clustering". Strandberg (1960, pp. 1319 and 1320) has suggested that the fact that the paramagnetic line widths in dilute ruby are greater than expected is due to a tendency of the chromium ions to cluster in groups instead of being randomly distributed. For a given average concentration c , any clustering must increase the average of c^2 and of c^2w_c . Thus, a measurement of the temperature variation of the maser effect at $\theta=29^\circ$, which, as we have shown, effectively measures c^2w_c , would provide valuable contributory evidence of clustering and of its variation with annealing and other processes.

VIII. ACKNOWLEDGMENTS

We are indebted to Mr. D. K. Milne for the construction of equipment and for assistance in the performance of the measurements, and to Professor N. Bloembergen who first suggested to us that our experiments could be explained in terms of cross relaxation.

IX. REFERENCES

- ARAMS, F. R., and OKWIT, S. (1959).—*Proc. Inst. Radio Engrs., N.Y.* **47**: 992.
 AUTLER, S. H., and McAVOY, N. (1958).—*Phys. Rev.* **110**: 280.
 BLOEMBERGEN, N. (1956).—*Phys. Rev.* **104**: 324.
 BLOEMBERGEN, N., SHAPIRO, S., PERSHAN, P. S., and ARTMAN, J. O. (1959).—*Phys. Rev.* **114**: 445.
 BOGLE, G. S., and SYMMONS, H. F. (1959).—*Aust. J. Phys.* **12**: 1.
 BOWERS, K. D., and OWEN, J. (1955).—*Rep. Progr. Phys.* **18**: 304.
 GEUSIC, J. E., SCHULZ-DU BOIS, E. O., DEGRASSE, R. W., and SCOVIL, H. E. D. (1959).—*J. Appl. Phys.* **30**: 1113.

- HOWARTH, D. J. (1958).—Royal Radar Establishment Memo. No. 1525.
 KIKUCHI, C., LAMBE, J., MAKHOV, G., and TERHUNE, R. W. (1959).—*J. Appl. Phys.* **30**: 1061.
 MIMMS, W. B., and MCGEE, J. D. (1960).—*Phys. Rev.* **119**: 1233.
 PACE, J. H., SAMPSON, D. F., and THORP, J. S. (1960a).—*Phys. Rev. Letters* **4**: 18.
 PACE, J. H., SAMPSON, D. F., and THORP, J. S. (1960b).—Royal Radar Establishment Memo. No. 1693.
 SHAPIRO, S., and BLOEMBERGEN, N. (1959).—*Phys. Rev.* **116**: 1453.
 STRANDBERG, M. W. P. (1960).—*Proc. Inst. Radio Engrs., N.Y.* **48**: 1307.
 VAN VLECK, J. H. (1940).—*Phys. Rev.* **57**: 426.
 WEBER, J. (1959).—*Rev. Mod. Phys.* **31**: 681.

APPENDIX

Derivation of the Rate Equation in the Presence of Cross-relaxation Processes

It has been shown by Bloembergen (1956) that the rate equation for, say, level 3 is, disregarding cross relaxation,

$$\frac{dn_3}{dt} = \sum_{j \neq 3} w_{j3}(n_j - n_3) + \frac{N\hbar\nu_{j3}}{4kT} + \sum_{j \neq 3} W_{j3}(n_j - n_3), \quad (\text{A1})$$

where the w 's and W 's are respectively spin-lattice relaxation rates and radiation-induced rates.

The contribution from cross-relaxation processes will now be derived. We shall confine ourselves to the situation in which $2(E_4 - E_3) = E_2 - E_1$, which is the case in ruby at low fields when $\theta = 29^\circ$. The following argument is intended to be read with the help of Figure 4 in the text.

If an ion is in level 3 and is at the lattice site α (Fig. 4 (a)), let us ask what is the probability of the cross-relaxation process shown diagrammatically in Figure 4 (b). (We disregard the inverse process for the meantime.) The process can occur only if sites β and γ (Fig. 4 (a)) are each filled with paramagnetic ions, and the chance of this is c^2 , where c is the concentration of paramagnetic ions in the crystal. If β is filled, the chance that it is correctly filled with an ion in state 2 is n_2/N (for $N = n_1 + n_2 + n_3 + n_4$); and similarly the chance that γ is correctly filled is n_3/N . Thus $c^2 n_2 n_3 / N^2$ is the probability that the appropriate situation exists. Let the probability per second of a cross-relaxation transition under these circumstances be $w_{\alpha\beta\gamma}$; $w_{\alpha\beta\gamma}$ depends on quantum-mechanical variables and on the displacements of β and γ from α . The transition probability associated with these particular sites is then $w_{\alpha\beta\gamma} c^2 n_2 n_3 / N^2$, and to dispose of the contribution of site α we must sum over all sites β and γ by replacing $w_{\alpha\beta\gamma}$ by

$$w_\alpha = \sum_{\beta\gamma} w_{\alpha\beta\gamma}.$$

As w_α is not necessarily the same for all sites α , let w_c be its average over unit cell of the crystal lattice; then the total number of transitions in the crystal becomes

$$n_3 \cdot w_c c^2 n_2 n_3 / N^2.$$

Remembering now the inverse transitions, the net number of transitions is seen to be $c^2 w_c (n_2 n_3^2 - n_1 n_4^2) / N^2$. The effect of these transitions may now be added to equation (A1), noting that each transition takes one ion from level 2 to 1 but two ions from 3 to 4. Thus the rate equation for level 3 is

$$\frac{dn_3}{dt} = \sum_{j \neq 3} w_{j3} (n_j - n_3) + \frac{N h \nu_{j3}}{4kT} + \sum_{j \neq 3} W_{j3} (n_j - n_3) + 2c^2 w_c (n_1 n_4^2 - n_2 n_3^2) / N^2.$$

The above treatment shows that $c^2 w_c / 16$ is the quantity which has the same kind of significance as w_{ij} . For just as w_{ij} is the number of spin-lattice processes in one direction per ion per second, so is $c^2 w_c n_2 n_3 / N^2$ the number of cross-relaxation processes in one direction per ion per second, and $n_2 n_3 / N^2 \simeq 1/16$.